Potential pitfalls of the early-time dynamics in two-dimensional electronic spectroscopy

Paleček, David; Edlund, Petra; Gustavsson, Emil; Westenhoff, Sebastian; Zigmantas, Donatas

Potential pitfalls of the early-time dynamics in two-dimensional electronic spectroscopy

David Paleček, Petra Edlund, Emil Gustavsson, Sebastian Westenhoff, and Donatas Zigmantas

View Online   Export Citation   CrossMark

ARTICLES YOU MAY BE INTERESTED IN

The Journal of Chemical Physics

Submit Today

The Emerging Investigators Special Collection and Awards
Recognizing the excellent work of early career researchers!

Potential pitfalls of the early-time dynamics in two-dimensional electronic spectroscopy

David Paleček,[1,2,a),b)] **Petra Edlund,**[3] **Emil Gustavsson,**[3] **Sebastian Westenhoff,**[3] **and Donatas Zigmantas**[1,c)]

AFFILIATIONS

[1] Department of Chemical Physics, Lund University, P.O. Box 124, SE-22100 Lund, Sweden
[2] Department of Chemical Physics, Charles University in Prague, Ke Karlovu 3, 121 16 Praha 2, Czech Republic
[3] Department of Chemistry and Molecular Biology, University of Gothenburg, Box 462, SE-40530 Gothenburg, Sweden

[a)] **Electronic mail:** dp602@cam.ac.uk
[b)] **Current address:** Cavendish Laboratory, University of Cambridge, JJ Thomson Avenue, Cambridge CB3 0HE, United Kingdom.
[c)] **Electronic mail:** donatas.zigmantas@chemphys.lu.se

ABSTRACT

Two-dimensional electronic spectroscopy, and especially the polarization-controlled version of it, is the cutting edge technique for disentangling various types of coherences in molecules and molecular aggregates. In order to evaluate the electronic coherences, which often decay on a 100 fs time scale, the early population times have to be included in the analysis. However, signals in this region are typically plagued by several artifacts, especially in the unavoidable pulse overlap region. In this paper, we show that, in the case of polarization-controlled two-dimensional spectroscopy experiment, the early-time dynamics can be dominated by the "incorrect" pulse ordering signals. These signals can affect kinetics at positive times well beyond the pulse overlap region, especially when the "correct" pulse ordering signals are much weaker. Moreover, the "incorrect" pulse ordering contributions are oscillatory and overlap with the spectral signatures of energy transfer, which may lead to misinterpretation of "incorrect" pulse ordering signals for fast-decaying coherences.

Published under license by AIP Publishing. https://doi.org/10.1063/1.5079817

I. INTRODUCTION

Controlling the motion of electrons in complex materials on a microscopic scale in a coherent fashion is one of the great scientific challenges for the future.[1] The important step, however, is to develop experimental and theoretical approaches for understanding the collective behavior of the electrons in molecular and condensed matter systems. Two-dimensional electronic spectroscopy (2DES) is a well-suited tool to investigate the coherent motions of both nuclei and electrons with sufficient concurrent spectral and time resolution.[2] For more than a decade, observation of pure electronic beatings, corresponding to the superposition of the excited electronic states and lasting for several hundreds of femtoseconds, has been claimed for the light-harvesting protein complexes.[3–6] Only recently, new theoretical approaches and experimental results started unraveling complex interactions between nuclear and electronic motions after impulsive excitation, pointing to a dominant role of

vibrations in the observed long-lived beatings.[7–12,42] Indeed, the very recent transient absorption and 2DES experimental findings support these theoretical predictions.[13–16]

In the case of coherences excited via transitions involving vibronically coupled states, the time-domain signals present evidence of mixing of electronic and vibrational degrees of freedom. To this end, polarization control of individual laser pulses in the 2DES experiment proved to be a very powerful method,[5,17] since it has the ability to disentangle excitonic coherences and coherences excited via vibronically coupled transitions from the purely vibrational ones excited via the Franck-Condon transitions.[13,15,18] To facilitate the correct interpretation of the subtle coherence signals, data have to be as free from artifacts as possible.

2DES can be regarded as an extension of the transient absorption spectroscopy, and both methods measure the third order nonlinear response of the sample. Numerous attempts to understand possible artifacts occurring in transient absorption measurements,

such as cross-phase modulation, spectral chirp and stimulated Raman signals, predominantly occurring during the pulse overlap, led to a mostly qualitative understanding of these artifacts for a given experimental configuration and a sample at hand. Yet, the understanding of these issues has not reached a rigorous quantitative level, nor provided ways to completely avoid them.[19–21] In 2DES, the situation regarding the artifacts is even more complicated given that (i) 2DES is often a fully resonant experiment in respect to excitation and detection frequencies, which adds all sorts of scattering contributions to the signal and (ii) due to four-wave mixing nature of 2DES, unlike in the transient absorption spectroscopy, it is impossible to get a "clean" zero population time signal, because of the unavoidable situation during the pulse overlap, when the desired multipulse sequence order cannot be "enforced," and thus multiple signals always contribute. The "incorrect" pulse ordering signals can be appreciable even beyond the "ideal" pulse overlap region, because of the imperfect pulse time profiles, and thus can interfere with the signals of interest. It is worth adding that whereas in transient absorption negative population, time signal outside the pulse overlap region is usually equal to zero, this is not the case for 2DES, as some "unwanted" signals contribute at negative population times within the decoherence time of the system.

Previous studies on potential artifacts in 2DES experiments have included propagation effects of the pulses,[22] phase matching and beam geometry,[23] and spectral chirp.[24] All these works focused on the lineshape distortions, and to the best of our knowledge, there is no study of possible artifacts regarding the oscillating signals (coherence phenomena) close to time zero. Thus, there is a clear need to gain a better understanding of these artifacts and identify the time regions where they can be ignored.

Several recent studies have focused on the initial times of the 2DES signal and proposed interpretations of the new phenomena at play. Meneghin *et al.* suggested that coherent energy transfer occurs in the light-harvesting peridinin-chlorophyll *a*-protein from rapidly decaying coherent oscillations with ~20 fs time constant.[25] Jun *et al.* supported assignment of the electronic coherences in chlorosomes by fitting an oscillatory component of the data with a 60 fs dephasing time.[26] Fast decaying electronic coherences have also been identified in quantum dots with retrieved dephasing times shorter than 25 fs.[27] None of these studies, however, provided an analysis of the possible early population time artifacts.

We do not aim to present an exhausting description of all the artifacts in 2DES, but rather we would like to initiate the discussion on the subject. Hence, we describe one of the artifacts, namely, "incorrect" pulse ordering effect, and analyze it specifically in the polarization-controlled 2DES experiment. We show that this artifact is observed well outside of the pulse overlap region and can be stronger than the generally weak coherence signals from the standard pulse ordering. We illustrate the contribution of the "incorrect" pulse sequence signals in the study of the photosynthetic reaction center from purple bacteria and argue that the problem could be ubiquitous. Therefore, the issue has to be taken into account whenever analyzing initial 100 fs of the coherence dynamics, especially in the polarization-selective 2DES experimental schemes, which are used to reveal weak signals of interest by suppressing otherwise dominating contributions.

II. MATERIALS AND METHODS

We employed a passively stabilized 2DES setup as described previously.[28,29] Briefly, a lab-made noncollinear parametric optical amplifier, pumped by the 1027 nm Pharos laser (Light Conversion Ltd.), was used to generate ~17 fs laser pulses, centered at 770 nm, with a FWHM of ~105 nm. Pulses were split into four replicas using a plate beamsplitter and transmissive diffraction grating. A spherical concave mirror was used to focus the three excitation beams and the fourth, so called local oscillator (LO) beam, attenuated by the 2 optical density (OD) filter, to the ~160 μm diameter spot on the sample. The first two beams were simultaneously chopped by optomechanical choppers, operating at different frequencies, and a double frequency modulation lock-in scheme was used for detection.[28] Interferograms between signal and LO were continuously detected by the CCD camera (PIXIS, Princeton Instruments). Polarizations of all the excitation pulses were independently set by the λ/4 waveplate and four wire-grid polarizers (contrast ratio > 800).

For all polarization-resolved 2DES experiments, an excitation energy of 4 nJ/pulse was used and coherence time was scanned from −171 to 270 fs with the 1.5 fs step. The following ranges of population time scans were used: (i) −300 fs to 60 fs for the ($\pi/4$, $-\pi/4$, $\pi/2$, 0) sequence in the negative time scan, (ii) 0–1800 fs for the ($\pi/4$, $-\pi/4$, $\pi/2$, 0) sequence in the positive time scan, and (iii) −300 fs to 600 fs for the ($\pi/4$, $\pi/2$, $-\pi/4$, 0) sequence. The 2D spectrum of all-parallel polarization was recorded at 2 nJ/pulse, 48 fs population delay with a coherence step of 1.75 fs over the population time range from −185.25 fs to 290.5 fs. The population time step was 12 fs in all experiments.

Mutated bacterial reaction centers (bRC) denoted W(L100)F, where tryptophan (W) protein residue on position L100 was exchanged with phenylalanine (F), were produced in the native *Rhodobacter sphaeroides* bacteria, grown under semianaerobic dark conditions at 30 °C and purified according to Ref. 30 with the following modifications. The solubilization of LDAO concentration was increased to 4% and the time to 3 h. Ion-exchange chromatography was performed with a toyopearl DEAE-650M column, and protein was eluted with a continuous 0–500 mM NaCl gradient. The protein was concentrated and flash frozen with liquid nitrogen. To oxidize bRC special pair, potassium ferricyanide [$K_3Fe(CN)_6$] in the resulting concentration of 150 mM was used. Samples were mixed with glycerol at the 35:65 (v/v) ratio in the 0.5 mm fused silica cell and cooled down to 77 K in a bath liquid nitrogen cryostat (Optistat DN, Oxford instruments). The concentration of the bRC was chosen such that the optical density was 0.2–0.3 at 800 nm under measurement conditions.

III. RESULTS AND DISCUSSION

A. Polarization-controlled 2D electronic spectroscopy

As evident from the previous investigations, when excited by ultrashort laser pulses, bacterial reaction centers (bRC) manifest various oscillatory patterns.[13,17,31–33] Polarization-controlled experiments on bRC have provided valuable insights into the coherent dynamics phenomena, and vibrational coherences, as well as coherences excited via vibronically coupled transitions have been reported.[13,17,33,34] For distinguishing different origins of coherences, the most effective scheme is the double-crossed (DC) polarization

sequence, where relative polarizations for the beams ($\vec{k}_1 - \vec{k}_4$), corresponding to the three excitation pulses, and the signal are set to ($\pi/4$, $-\pi/4$, $\pi/2$, 0), respectively.[5,17,34,35] In this way, it is possible to suppress both the population-related and purely vibrational Franck-Condon coherence signals up to 125 times, which sharply enhances sensitivity for detecting generally weak coherences excited via vibronically coupled transitions.[13,15] To investigate the effect of the "incorrect" pulse ordering, we extended the DC experimental scan to negative population times.

B. Pulse ordering in the 2DES experiments: appearance of fringes in the negative population time spectra

For each population time t_2, 2DES correlates excitation and detection frequencies, which are conjugated Fourier transform pairs of the coherence time delay t_1 and detection time delay t_3. The former is the delay between the first two excitation pulses, and the latter is the arrival time of the signal after the third excitation pulse.[2] Figure 1(a) illustrates how the pulses are scanned during the 2DES data acquisition in our laboratory. For each coherence scan, the population time t_2 is fixed and the coherence time delay t_1 is varied by scanning the $\vec{k}_1$ pulse ($t_1 > 0$, rephasing part) or $\vec{k}_2$ pulse [$t_1 < 0$, nonrephasing (NR) part] before time zero with an interferometric precision. Time delay t_{LO} between the $\vec{k}_3$ pulse and the local oscillator ($\vec{k}_4$) is kept always constant (the LO arrives at $t_{LO} \sim 2.5$ ps after

the $\vec{k}_3$ pulse), and for varying population time t_2, the $\vec{k}_3$ and $\vec{k}_4$ pulse pair is delayed.

For a given negative population time $t_2 < 0$, the coherence time scans yield four separate pulse orderings [see Fig. 1(c)]. Scanning rephasing part for $t_1 > |t_2|$ leads to $-\vec{k}_1 + \vec{k}_3 + \vec{k}_2$ rephasing type (R type) sequence as depicted in Figs. 1(b) and 1(c). As the $\vec{k}_1$ pulse passes over the $\vec{k}_3$ pulse ($0 < t_1 < |t_2|$), the sequence changes to the nonrephasing type (NR type): $\vec{k}_3 - \vec{k}_1 + \vec{k}_2$. Note that in this pulse sequence every t_1 step changes the effective population time, since $\vec{k}_1$ defines the effective time zero. Analogous analysis can be performed on the nonrephasing scan ($t_1 < 0$), which contributes to the total signal with the double quantum coherence type (DQC type) pathways [see Fig. 1(c)].[36,37]

The strongest negative population time signal for the rephasing scan ($t_1 > 0$) is emitted when $\vec{k}_1, \vec{k}_3$ overlap in time, which corresponds to $t_1 = |t_2|$ and $t_3 = t_3' + |t_2|$ [see Fig. 1(b)]. This is clearly visible in the time domain 2D representation (t_1, t_3) signal, where the inverse Fourier transform was carried out for the detection frequency ω_3 (Fig. 2). It can also be seen that as t_2 gets more negative the signal shifts along the diagonal toward larger t_1 and t_3. On the other hand, the strongest signal for the nonrephasing scan ($t_1 < 0$) is expected for $t_1 = -|t_2|$ and $t_3 = t_3' + |t_2|$, which means that DQC type signals shift in the antidiagonal direction as t_2 gets more negative. No such signal is observed in Fig. 2, therefore we conclude that DQC signals coming from the nonrephasing scan contribute negligibly to the presented data, and the observed negative population time signal is dominated by the rephasing scan contributions.

Different values of t_1, t_3' for the $t_2 < 0$ measurements, as compared to the normal ordering in the $t_2 > 0$ measurements are expected to cause spectral fringes along the corresponding frequency axes ω_1 and ω_3 according to the Fourier shift theorem. As the t_2 delay becomes more negative, the spectral fringes get denser as observed in Fig. 2. In the time domain 2D representation (t_1, t_3), the signal shifts in respect to both t_1 and t_3 by a time delay equal to $|t_2|$, and therefore the fringes in the resulting 2D spectra appear in both horizontal (ω_1) and vertical (ω_3) directions (thus in parallel to the diagonal). The necessity of taking these signals into account in coherence dynamics studies arises from the fact that they are oscillatory in nature. The spectral fringes are t_2-dependent, as they get denser with increasingly negative t_2, which effectively leads to appearance of oscillatory time traces, which also extend to the positive population times, as discussed in detail below.

C. Effect of polarization

For the polarization-controlled 2DES of isotropic samples, each of the possible interaction (Liouville) pathways has an orientational prefactor, which contains scalar products of the transition dipole moments and unit vectors of the polarized electric fields.[35,38] If we assume two molecular transition dipole moments (A, B) with a nonzero angle between them, the four electromagnetic fields can interact either with only one of the dipoles (AAAA and BBBB) or both (AABB, ABAB, and ABBA). Note that for brevity we omit the "symmetric" pathways where A and B are interchanged. AAAA and AABB pathways correspond to population dynamics and Franck-Condon vibrational coherences, whereas the ABAB and
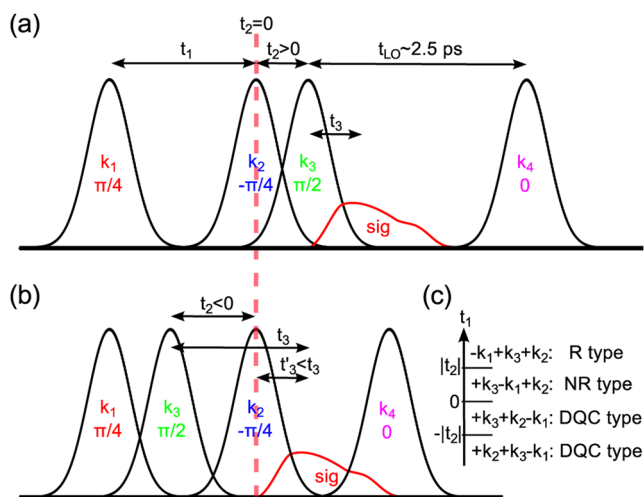

FIG. 1. Two pulse sequences as considered in the text. (a) Double-crossed polarization experiment ($\pi/4$, $-\pi/4$, $\pi/2$, 0) specifically filters electronic coherences and coherences excited via vibronically coupled transitions. For a given population time t_2, the $\vec{k}_1$ ($\vec{k}_2$) pulse is scanned to obtain rephasing (nonrephasing) part of the 2D spectra. (b) The "incorrect" pulse ordering sequence for the negative population time experiment ($\pi/4$, $\pi/2$, $-\pi/4$, 0), where pulses $\vec{k}_2$ and $\vec{k}_3$ switch places, was identified as the source of the strong signal for $t_2 < 0$ during the pulse overlap and even beyond. (c) For a given negative population time $t_2 < 0$, scanning the coherence time yields four distinct pulse orderings which can be categorized into rephasing ($-\vec{k}_1 + \vec{k}_3 + \vec{k}_2$), nonrephasing ($+\vec{k}_3 - \vec{k}_1 + \vec{k}_2$), and double quantum coherence (DQC) pathways ($\vec{k}_3 + \vec{k}_2 - \vec{k}_1$, $\vec{k}_2 + \vec{k}_3 - \vec{k}_1$).
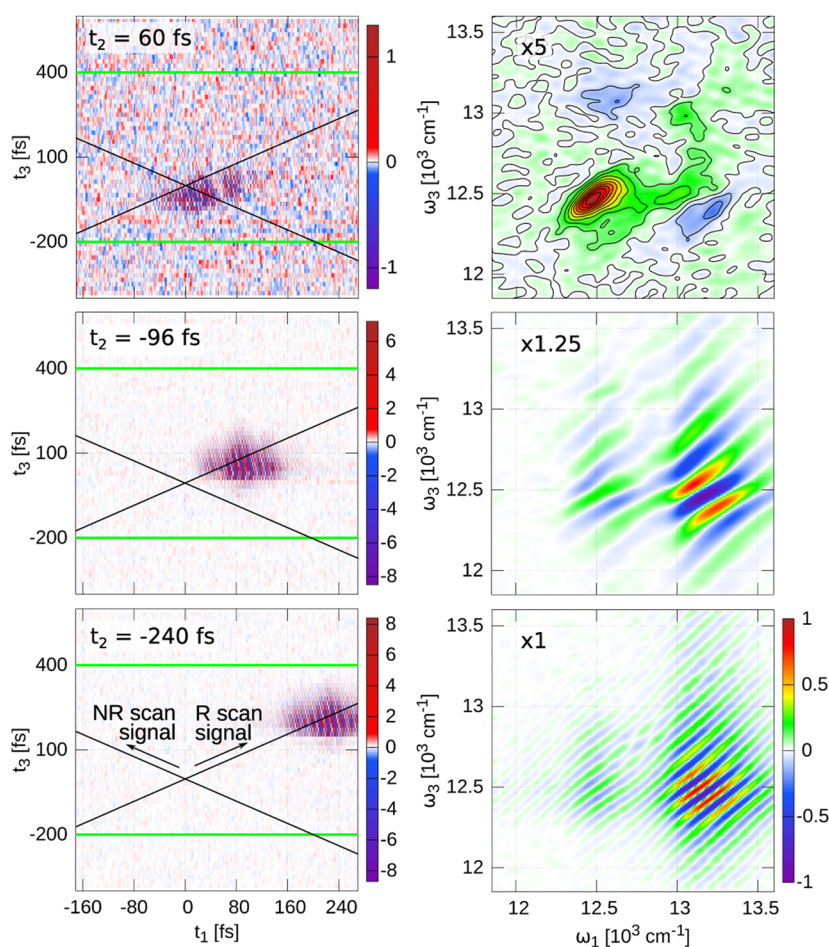
FIG. 2. 2D time domain (t_1, t_3) signals (left column) for several population times of the DC experiment, together with the extracted total real (absorptive) 2D spectra (right column), all phased according to $t_2 > 0$. Green lines in the left column mark the full width half maximum of the Fourier window filter applied in the detection time t_3. For $t_2 < 0$, signal shifts by $|t_2|$ along both t_1 and t_3 time axes, and therefore the fringes in the resulting 2DES spectra (right column) appear in parallel to the diagonal. Each spectrum is normalized to the maximum signal, with relative scaling factors shown in the top left corner of each 2D spectrum.

ABBA pathways represent electronic coherences, as well as coherences excited via vibronically coupled transitions. For photosynthetic systems containing chlorophyll-type molecules, the latter coherence signals are weak compared to the population and vibrational coherence signals, which, on the other hand, are well suppressed for all the angles between the dipole moments in the DC measurement (see Fig. 3, blue).[13,15] In this way, the DC experiment enhances the sensitivity toward the electronic coherences and coherences excited via vibronically coupled transitions. However, the "incorrect" pulse ordering for $t_2 < 0$ alters the DC polarization sequence—for the rephasing scan—to ($\pi/4$, $\pi/2$, $-\pi/4$, 0) and ($\pi/2$, $\pi/4$, $-\pi/4$, 0) [see Fig. 1(c)]. These polarization sequences exhibit different prefactors for Liouville pathways (see Fig. 3, green) and do not filter out the AABB signals. These signals notably include energy transfer pathways that manifest as stimulated emission signals at the cross-peaks (CP) below the diagonal. The amplitude of these signals near the $t_2 = 0$ (depending on the energy transfer efficiency and the rise and decay rates of the cross-peaks) defines the relative ratio of the "incorrect" pulse ordering signals to the coherences excited via vibronically coupled transitions in the DC measurement.

D. "Incorrect" pulse ordering: Signal shape and origin

It can be easily seen in the negative population time spectra presented in Fig. 2 that the strongest signal amplitude appears at the below diagonal cross-peak, suggesting the energy transfer origin of the "incorrect" pulse ordering signal. To assign the shape and dynamics of this signal, we performed an additional 2DES experiment, where we rearranged the original DC scheme to ($\pi/4$, $\pi/2$, $-\pi/4$, 0). Based on the polarization arguments presented in Sec. III C, it can be found that the ($\pi/4$, $\pi/2$, $-\pi/4$, 0) polarization scheme is mostly sensitive to the energy transfer pathways, electronic coherences, and coherences excited via vibronically coupled transitions. This is demonstrated in Fig. 4(a), which compares all-parallel and ($\pi/4$, $\pi/2$, $-\pi/4$, 0) 2D spectra. Figure 4(b) shows a kinetic trace from the below diagonal cross-peak of the energy transfer-specific polarization scheme ($\pi/4$, $\pi/2$, $-\pi/4$, 0), with fitted time constants describing energy transfer between the excitonic states within the reaction center (80 fs) and subsequent decay of the stimulated emission signal (400 fs). By carefully considering the pulse orderings in this and DC experiments, it becomes evident that the negative time signal for the ($\pi/4$, $\pi/2$, $-\pi/4$, 0) polarization sequence corresponds to the artifact
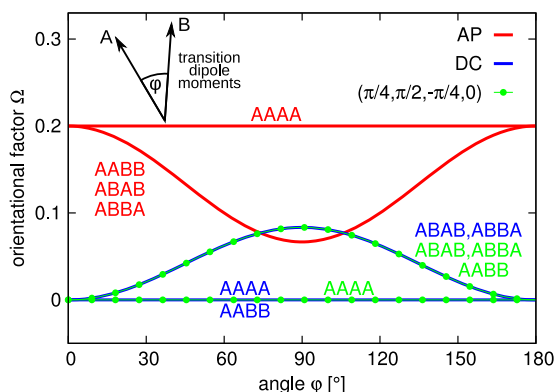
FIG. 3. Dependence of the orientational prefactor on the angle φ between the transition dipole moments A and B for the selected polarization schemes in 2DES experiments. Two contributions stem from population dynamics and/or vibrational coherence (AAAA and AABB) and another two—from electronic coherences or from coherences excited via vibronically coupled transitions (ABAB and ABBA). For all parallel scheme (AP, red), all pathways contribute to the 2DES signal. The DC polarization scheme is selective as most pathways vanish for all possible angles φ, whereas ABAB and ABBA (blue) remain. In the case of the "incorrect" pulse ordering sequences, in addition to all the pathways that survive the DC sequence, e.g., the energy transfer pathways (AABB, green) also remain.

of the $(\pi/4, -\pi/4, \pi/2, 0)$ sequence at positive time delays. This clearly demonstrates that (i) the "incorrect" pulse ordering signal in the DC experiment contributes predominantly to the below diagonal cross-peak, (ii) it plagues the first 100 fs of the DC sequence as marked by the red shaded area in Fig. 4(b), and (iii) this signal stems from the energy transfer pathway, as evidenced by the location of this signal in the 2D spectra (Figs. 2 and 4) and the polarization selectivity of the $(\pi/4, \pi/2, -\pi/4, 0)$ sequence. The amplitude of the "incorrect" pulse ordering signal leaking into the $t_2 \geq 0$ DC measurement is directly related to the amplitude of the energy transfer signal near $t_2 = 0$ [Fig. 4(b)], which depends on the energy transfer efficiency as well as rise and decay rates of the corresponding cross-peak [see Fig. 4(b)].

The spectral location of the $t_2 < 0$ signal in the DC measurement map is significant, since the lower cross-peak has been often analyzed in relation to coherence beatings associated with the energy transfer dynamics in various light-harvesting systems.[3,4]

E. Time trace analysis

Here, we present the analysis of the $t_2 < 0$ signals showing the evidence that the oscillations in the polarization-controlled 2D spectra at close to zero population time are dominated by the "incorrect" pulse ordering contributions, which can extend up to ~+100 fs.
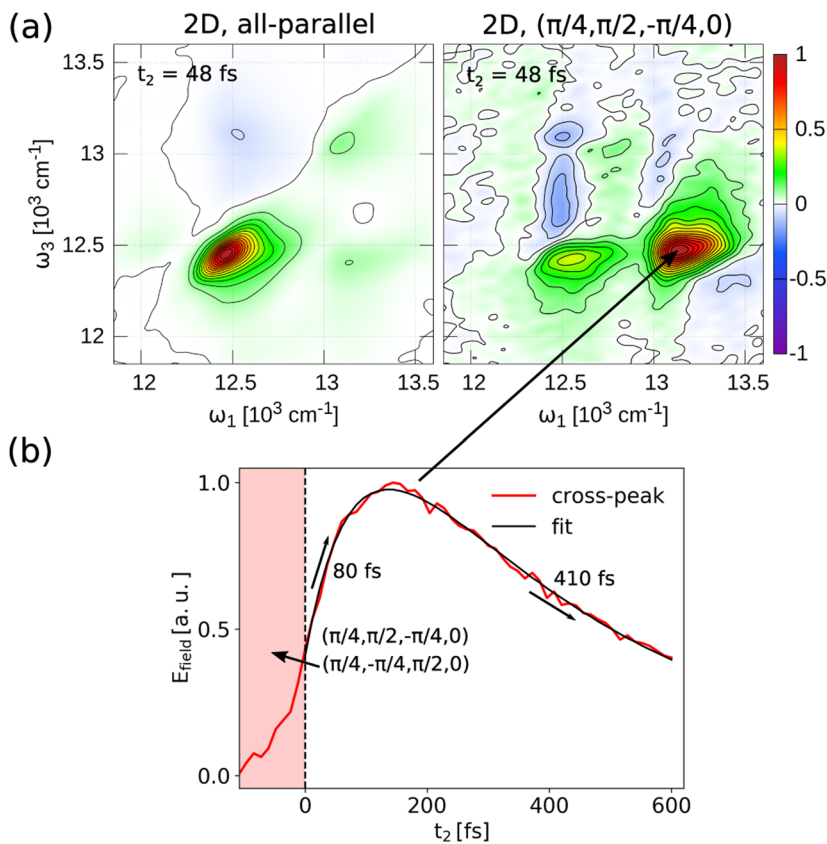
FIG. 4. (a) Comparison of the total real 2D spectra for all-parallel (left) and $(\pi/4, \pi/2, -\pi/4, 0)$ sequence (right), which is selective toward the energy transfer pathways and it is also found as a main source of the "incorrect" pulse ordering signal in the DC experiment. (b) Kinetic trace of the below diagonal cross-peak extracted from the $(\pi/4, \pi/2, -\pi/4, 0)$ sequence. The negative time signal (shaded in red) represents the artifact signal "leaking" into the positive $t_2 > 0$ times in the DC sequence.

Figure 5 shows time domain traces from the cross-peaks in the DC measurement for $t_2 = -300 \rightarrow 60$ fs together with the overlaid traces from the positive population time measurement for $t_2 = 0 \rightarrow 500$ fs. It is evident from the overlap of the two independent measurements that the oscillating signals are highly reproducible. Clearly, the oscillation signal at $t_2 < 0$ below the diagonal is much stronger than the one above the diagonal, which is expected from the position of the "incorrect" pulse ordering signal on the 2D map (see Figs. 2 and 4). Closer inspection of the below diagonal cross-peak signal at early times (inset of Fig. 5) allows us to conclude that with the ~17 fs-pulses (autocorrelation of ~24 fs), first ~100 fs of the kinetic traces at this spectral position are distorted due to the "incorrect" pulse ordering. We estimate that the "incorrect" pulse ordering signal is ~5 times stronger at $t_2 = 0$ fs than the "real" coherences. However, it is difficult to account for such pronounced signals well beyond the cross correlation time. Therefore, we infer that a nonideal pulse shape, such as "wing(s)" in the temporal profile of the laser pulses, provides sufficient light intensity for "incorrect" pulse ordering signals to extend beyond the pulse cross correlation time. We estimate that in the experiments presented here the intensity profile wings were below 8% of the main pulse. Such and similar temporal profile features are very common when working with sub-20 fs pulses.

F. Potential interference of the artifact signals with coherences

Performing Fourier transform over t_2 time for each point in the 2D spectra and plotting oscillation maps allows for visualization of the oscillatory amplitudes in 2D spectra.[13,39,40] Integrating the Fourier amplitude of the obtained oscillation maps provides information about the overall dominant frequencies, which are presented for bRC in Fig. 6. The Fourier amplitude spectrum for $t_2 = -276 \rightarrow 0$ fs features a broad peak around $\omega_2 = -700$ cm^{-1} which reflects the spectral fringes generated in dependence on the spectral
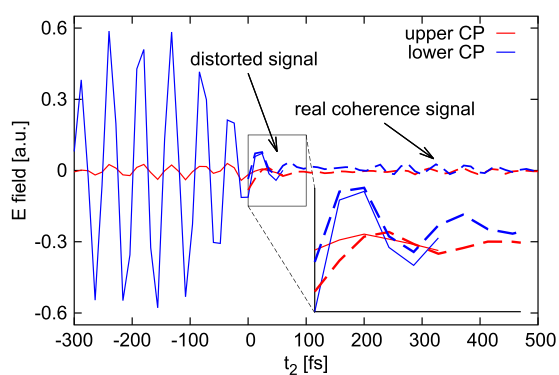

FIG. 5. Single point t_2 kinetic traces for the lower (blue) and upper (red) cross-peaks (CPs) extracted from the DC measurements. The inset shows a close up on the first 100 fs. The lower cross-peak oscillates strongly in the negative t_2 times, which influences also the first ~100 fs of the positive t_2, as the "real" coherence signals are expected to have comparable amplitude in this range (see text for details). Positive population time measurement traces (dashed lines) are overlaid with the negative time measurement traces (solid lines) for the first 60 fs.
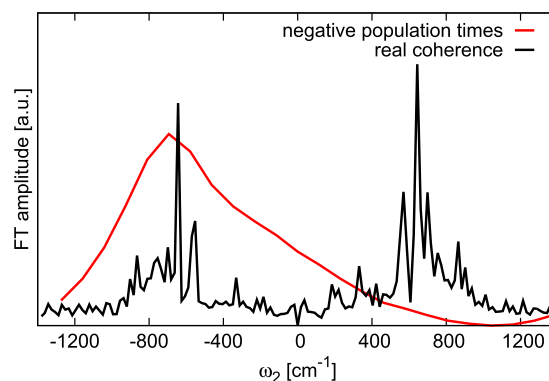

FIG. 6. Integrated Fourier amplitudes of oscillation frequencies within the 2D spectra. (Red) Negative population time Fourier amplitudes obtained from the DC measurement for $t_2 = -276 \rightarrow 0$ fs. (Black) "Real" coherence Fourier amplitudes, extracted from the independent DC measurement for $t_2 = 0 \rightarrow 1800$ fs, are shown for comparison.

distance of the cross-peak from the diagonal, as well as the extent of the negative population times measured. Importantly, the frequencies of the "real" coherence signals (Fourier transform of the $t_2 = 0 \rightarrow 1800$ fs measurement) overlap with those of the "incorrect" pulse ordering "oscillations" for $t_2 < 0$. Therefore, the oscillating signals from "incorrect" pulse ordering could be misinterpreted as "real" coherences, or at least distort their appearance.

It is worth noting that the relative strength of the "incorrect" pulse ordering signal strongly depends on the phase stability of the 2DES setup, since the reverse order of the $\vec{k}_2(\vec{k}_1)$ and $\vec{k}_3$ pulses makes the "incorrect" pulse ordering prone to possible phase instabilities between pulse pairs $\vec{k}_1$, $\vec{k}_2$ and $\vec{k}_3$, $\vec{k}_4$.[41] Here we see an opportunity to experimentally minimize the "incorrect" ordering effects by introducing random phase variations to t_2, while keeping the phase stability within the pulse pairs $(\vec{k}_1, \vec{k}_2)$ and $(\vec{k}_3, \vec{k}_4)$. We also emphasize here that the upper cross-peak contains minimal contribution from the "incorrect" pulse ordering signals and it is therefore most suited for the analysis of the coherences in the DC measurements.[13]

As pointed out above, the "incorrect" pulse ordering signal, which gives rise to the artifact originates from the energy transfer related signals. These are present in all multichromophore molecular systems, including photosynthetic complexes, where coherence dynamics has been intensively studied. Thus, the phenomenon of the negative population time signals interfering with the coherence below the diagonal in the DC and likely other polarization-controlled 2DES experiments could be general for the multichromophore systems. However, the relative amplitudes of these two types of signals depend on the rate and efficiency of the energy transfer, as well as the amplitude of the coherences.

Here, we focused on the "incorrect" pulse ordering signal distorting early-time dynamics in the DC measurements, however, because of the general nature of the artifact, it is present for any polarization sequence, including the "standard" all parallel or magic angle 2DES measurements. That being said, in these "standard" measurements, the amplitude of the artifact is expected to be comparable to the real signals at $t_2 = 0$ fs. Therefore, the potential problem

is certainly present in the "ideal" pulse overlap region, but for realistic pulses featuring complex profiles, will also extend beyond this region.

IV. CONCLUSIONS

Technical advances in the phase stability, polarization control, and theoretical modeling have extended the analysis of the 2DES experiments to the short population times. This brings out the need for understanding the pulse overlap region in great detail in order to pinpoint short-lived coherence signals. To elevate the awareness of the pulse overlap artifacts and their potential effect on 2DES measurements, we analyze one of them, unraveling its physical origin and extent. We specifically address the "incorrect" pulse ordering effects for the double-crossed polarized pulse sequence, which filters coherences with electronic character and coherences excited via vibronically coupled transitions. The effect is found to dominate the pulse overlap region, but it also extends up to ~100 fs into the positive time delays for a certain 2DES spectral region, even when 17 fs pulses are used. We conclude that selective polarization sequences are particularly prone to "incorrect" pulse ordering artifacts when wings are present in the time profile of the used pulses. Importantly, the "incorrect" pulse ordering signals are oscillatory in nature, appearing predominantly below the diagonal in the 2D spectra with the oscillation frequencies similar to the modes typical for the systems containing chlorophyll-like molecules. Thus, such artifacts can be easily misinterpreted for rapidly decaying coherence beatings. With this example, we show that great care has to be taken when analyzing early population time signals in 2DES experiments.

REFERENCES

[1] G. R. Fleming and M. Ratner, "Grand challenges in basic energy sciences," Phys. Today **61**(7), 28 (2008).

[2] D. M. Jonas, "Two-dimensional femtosecond spectroscopy," Annu. Rev. Phys. Chem. **54**, 425–463 (2003).

[3] G. S. Engel, T. R. Calhoun, E. L. Read, T.-K. Ahn, T. Mančal, Y.-C. Cheng, R. E. Blankenship, and G. R. Fleming, "Evidence for wavelike energy transfer through quantum coherence in photosynthetic systems," Nature **446**, 782–786 (2007).

[4] E. Collini, C. Y. Wong, K. E. Wilk, P. M. G. Curmi, P. Brumer, and G. D. Scholes, "Coherently wired light-harvesting in photosynthetic marine algae at ambient temperature," Nature **463**, 644–647 (2010).

[5] G. S. Schlau-Cohen, A. Ishizaki, T. R. Calhoun, N. S. Ginsberg, M. Ballottari, R. Bassi, and G. R. Fleming, "Elucidation of the timescales and origins of quantum electronic coherence in LHCII," Nat. Chem. **4**, 389–395 (2012).

[6] H. Lee, Y. Cheng, and G. Fleming, "Coherence dynamics in photosynthesis: Protein protection of excitonic coherence," Science **316**, 1462 (2007).

[7] V. Butkus, D. Zigmantas, D. Abramavicius, and L. Valkunas, "Distinctive character of electronic and vibrational coherences in disordered molecular aggregates," Chem. Phys. Lett. **587**, 93–98 (2013).

[8] N. Christensson, H. F. Kauffmann, T. Pullerits, and T. Mančal, "Origin of long-lived coherences in light-harvesting complexes," J. Phys. Chem. B **116**, 7449–7454 (2012).

[9] V. Tiwari, W. K. Peters, and D. M. Jonas, "Electronic resonance with anti-correlated pigment vibrations drives photosynthetic energy transfer outside the adiabatic framework," Proc. Natl. Acad. Sci. U. S. A. **110**, 1203–1208 (2013).

[10] J. M. Womick and A. M. Moran, "Exciton coherence and energy transport in the light-harvesting dimers of allophycocyanin," J. Phys. Chem. B **113**, 15747–15759 (2009).

[11] J. M. Womick and A. M. Moran, "Vibronic enhancement of exciton sizes and energy transport in photosynthetic complexes," J. Phys. Chem. B **115**, 1347–1356 (2011).

[12] D. C. Arnett, C. C. Moser, P. L. Dutton, and N. F. Scherer, "The first events in photosynthesis: Electronic coupling and energy transfer dynamics in the photosynthetic reaction center from *Rhodobacter sphaeroides*," J. Phys. Chem. B **103**, 2014–2032 (1999).

[13] D. Paleček, P. Edlund, S. Westenhoff, and D. Zigmantas, "Quantum coherence as a witness of vibronically hot energy transfer in bacterial reaction center," Sci. Adv. **3**, e1603141 (2017).

[14] M. Maiuri, E. E. Ostroumov, R. G. Saer, R. E. Blankenship, and G. D. Scholes, "Coherent wavepackets in the Fenna–Matthews–Olson complex are robust to excitonic-structure perturbations caused by mutagenesis," Nat. Chem. **10**, 177–183 (2018).

[15] E. Thyrhaug, R. Tempelaar, M. J. P. Alcocer, K. Žídek, D. Bína, J. Knoester, T. L. C. Jansen, and D. Zigmantas, "Identification and characterization of diverse coherences in the Fenna–Matthews–Olson complex," Nat. Chem. **10**, 780–786 (2018).

[16] F. Novelli, A. Nazir, G. H. Richards, A. Roozbeh, K. E. Wilk, P. M. G. Curmi, and J. A. Davis, "Vibronic resonances facilitate excited-state coherence in light-harvesting proteins at room temperature," J. Phys. Chem. Lett. **6**, 4573–4580 (2015).

[17] S. Westenhoff, D. Paleček, P. Edlund, P. Smith, and D. Zigmantas, "Coherent picosecond exciton dynamics in a photosynthetic reaction center," J. Am. Chem. Soc. **134**, 16484–16487 (2012).

[18] V. P. Singh, M. Westberg, C. Wang, P. D. Dahlberg, T. Gellen, A. T. Gardiner, R. J. Cogdell, and G. S. Engel, "Towards quantification of vibronic coupling in photosynthetic antenna complexes," J. Chem. Phys. **142**, 212446 (2015).

[19] M. Lorenc, M. Ziolek, R. Naskrecki, J. Karolczak, J. Kubicki, and A. Maciejewski, "Artifacts in femtosecond transient absorption spectroscopy," Appl. Phys. B **74**, 19–27 (2002).

[20] D. Polli, D. Brida, S. Mukamel, G. Lanzani, and G. Cerullo, "Effective temporal resolution in pump-probe spectroscopy with strongly chirped pulses," Phys. Rev. A **82**, 053809 (2010).

[21] U. Megerle, I. Pugliesi, C. Schriever, C. F. Sailer, and E. Riedle, "Sub-50 fs broadband absorption spectroscopy with tunable excitation: Putting the analysis of ultrafast molecular dynamics on solid ground," Appl. Phys. B **96**, 215–231 (2009).

[22] H. Li, A. P. Spencer, A. Kortyna, G. Moody, D. M. Jonas, and S. T. Cundiff, "Pulse propagation effects in optical 2D Fourier-transform spectroscopy: Experiment," J. Phys. Chem. A **117**, 6279–6287 (2013).

[23] M. K. Yetzbacher, N. Belabas, K. A. Kitney, and D. M. Jonas, "Propagation, beam geometry, and detection distortions of peak shapes in two-dimensional Fourier transform spectra," J. Chem. Phys. **126**, 044511 (2007).

[24] P. F. Tekavec, J. A. Myers, K. L. M. Lewis, F. D. Fuller, and J. P. Ogilvie, "Effects of chirp on two-dimensional Fourier transform electronic spectra," Opt. Express **18**, 11015–11024 (2010).

[25] E. Meneghin, A. Volpato, L. Cupellini, L. Bolzonello, S. Jurinovich, V. Mascoli, D. Carbonera, B. Mennucci, and E. Collini, "Coherence in carotenoid-to-chlorophyll energy transfer," Nat. Commun. **9**, 3160 (2018).

[26] S. Jun, C. Yang, M. Isaji, H. Tamiaki, J. Kim, and H. Ihee, "Coherent oscillations in chlorosome elucidated by two-dimensional electronic spectroscopy," J. Phys. Chem. Lett. **5**, 1386–1392 (2014).

[27] M. B. Cassette Elsa, D. Pensack Ryan, and G. D. Scholes, "Room-temperature exciton coherence and dephasing in two-dimensional nanostructures," Nat. Commun. **6**, 6086 (2015).

[28] R. Augulis and D. Zigmantas, "Two-dimensional electronic spectroscopy with double modulation lock-in detection: Enhancement of sensitivity and noise resistance," Opt. Express **19**, 13126–13133 (2011).

[29] R. Augulis and D. Zigmantas, "Detector and dispersive delay calibration issues in broadband 2D electronic spectroscopy," J. Opt. Soc. Am. B **30**, 1770 (2013).

[30] M. Paddock, S. Rongey, E. Abresch, G. Feher, and M. Okamura, "Reaction centers from three herbicide-resistant mutants of *Rhodobacter sphaeroides* 2.4.1: Sequence analysis and preliminary characterization," Photosynth. Res. **17**, 75–96 (1988).

[31] I. S. Ryu, H. Dong, and G. R. Fleming, "Role of electronic-vibrational mixing in enhancing vibrational coherences in the ground electronic states of photosynthetic bacterial reaction center," J. Phys. Chem. B **118**, 1381–1388 (2014).

[32] P. D. Dahlberg, P.-C. Ting, S. C. Massey, E. C. Martin, C. N. Hunter, and G. S. Engel, "Electronic structure and dynamics of higher-lying excited states in light harvesting complex 1 from *Rhodobacter sphaeroides*," J. Phys. Chem. A **120**, 4124–4130 (2016).

[33] M. Vos, M. Jones, C. Hunter, J. Breton, J. Lambry, and J. Martin, "Coherent dynamics during the primary electron-transfer reaction in membrane-bound reaction centers of *Rhodobacter sphaeroides*," Biochemistry **33**, 6750–6757 (1994).

[34] D. Paleček and D. Zigmantas, "Double-crossed polarization transient grating for distinction and characterization of coherences," Opt. Express **26**, 32900–32907 (2018).

[35] R. Hochstrasser, "Two-dimensional IR-spectroscopy: Polarization anisotropy effects," Chem. Phys. **266**, 273–284 (2001).

[36] J. Kim, S. Mukamel, and G. D. Scholes, "Two-dimensional electronic double-quantum coherence spectroscopy," Acc. Chem. Res. **42**, 1375–1384 (2009).

[37] A. Nemeth, F. Milota, T. Mančal, T. Pullerits, J. Sperling, J. Hauer, H. F. Kauffmann, and N. Christensson, "Double-quantum two-dimensional electronic spectroscopy of a three-level system: Experiments and simulations," J. Chem. Phys. **133**, 094505 (2010).

[38] A. Zilian and J. C. Wright, "Polarization effects in four-wave mixing of isotropic samples," Mol. Phys. **87**, 1261–1272 (1996).

[39] V. Butkus, D. Zigmantas, L. Valkunas, and D. Abramavicius, "Vibrational vs electronic coherences in 2D spectrum of molecular systems," Chem. Phys. Lett. **545**, 40–43 (2012).

[40] H. Li, A. D. Bristow, M. E. Siemens, G. Moody, and S. T. Cundiff, "Unraveling quantum pathways using optical 3D Fourier-transform spectroscopy," Nat. Commun. **4**, 1390 (2013).

[41] T. Brixner, T. Mančal, I. V. Stiopkin, and G. R. Fleming, "Phase-stabilized two-dimensional electronic spectroscopy," J. Chem. Phys. **121**, 4221–4236 (2004).

[42] A. W. Chin, J. Prior, R. Rosenbach, F. Caycedo-Soler, S. F. Huelga, and M. B. Plenio, "The role of non-equilibrium vibrational structures in electronic coherence and recoherence in pigment–protein complexes," Nat. Phys. **9**, 113–118 (2013).